Solitary Waves and Fluctuations in Fragile Matter

Upadhyaya, N.

5

SOLITARY WAVE IN FLUCTUATING BACKGROUND

In linear elastic solids, phonons are the basic mechanical excitations responsible for energy propagation. By contrast, as discussed in the previous chapters, an aggregate of macroscopic grains just in contact with their nearest neighbours constitute a novel elastic material where solitary waves or shocks replace phonons as the basic excitations [32, 49, 26]. The origin of these strongly non-linear waves can be traced to the fact that, unlike the case of harmonic springs, the repulsive force between two grains in contact does not depend linearly on the relative compression. So far, little effort has been directed to determine the fate of these strongly non-linear excitations in a background of thermal fluctuations because temperature is clearly not a parameter relevant to the elastic response of macroscopic grains.

However, as we saw in chapter 4, an impulse excitation attenuates as it propagates through a two dimensional amorphous packing and interacts with the inhomogeneities. In turn, the aggregate of grains get effectively thermalized by the energy that leaks away from the solitary wave and the final state of the packing changes to a fluid-like state, suggesting the notion of a granular analogue of temperature. Unlike a system truly in thermal equilibrium, this new state is at best categorized as a quasi-equilibrium state since an analogous fluctuation-dissipation mechanism to maintain the state of equilibrium is so far not known to exist.

Notwithstanding, granular aggregates at zero pressure are just one example of a broader class of materials that can be prepared in a unique mechanical state called *sonic vacuum* [32]. Grafted colloidal particles [50] and ultra-cold atoms in optical lattices [51] are microscopic systems that allow for tunable non-linear interactions, while being naturally coupled to a source of fluctuation (thermal or quantum). Much like the granular analogue of temperature, these fluctuations restore rigidity and generate long wavelength phonon modes [52, 38]. However, the physics of very high amplitude strain propagation is still predominantly non-linear and resembles the state of sonic vacuum perturbed by background fluctuations. This extreme regime is

particularly relevant for energy transport in some biological systems, where transport occurs through localized non-linear excitations with energy significantly higher than the thermal energy [55, 56].

Moreover, systems such as polymer networks and colloidal glasses undergoing an unjamming transition are also characterized by vanishing elastic moduli as the coordination number or packing fraction are lowered towards the critical point [57]. The effect of thermal fluctuations on the *non-linear* response of materials undergoing an unjamming transition is relatively unexplored, despite they are obvious examples of a sonic vacuum state at zero temperature [53, 58, 59]. Note, that in the case of jamming the linear elastic moduli can be lowered towards zero even if the microscopic interactions are harmonic, simply because there are not enough forces to prevent floppy motions.

In this chapter, we now focus on strongly non-linear mechanical waves propagating in a background of small thermal fluctuations, a non-equilibrium problem that lies outside the realm of perturbation theory. The starting point of conventional perturbation methods is a linear elastic solid, possibly at finite temperature, perturbed by small anharmonic terms. By contrast, we adopt as a starting point the fully non-linear state of sonic vacuum whose elementary excitations are long-lived solitary waves [60]. Subsequently we *switch on* temperature as a small perturbation that creates a background of thermal fluctuations.

As a minimal model that is analytically tractable, we study impulse propagation in a one dimensional lattice of non-linear springs with a tune-able power law interaction. In addition to the compressive solitary waves seen in a lattice of macroscopic grains with one-sided repulsive interaction, we find an accompanying anti-solitary wave solution for the lattice of non-linear springs with two sided interactions. By coupling the lattice to a heat bath, we then study the effects of the thermal fluctuations on the leading solitary wave generated in response to an impulse of energy much higher than the background thermal energy. Our approach in a nutshell is to treat the solitary wave as a quasi-particle and derive an effective Langevin equation that describes its stochastic dynamics. We corroborate our analytical predictions for the damping rate and thermal diffusion of the solitary waves with Langevin dynamic simulations.

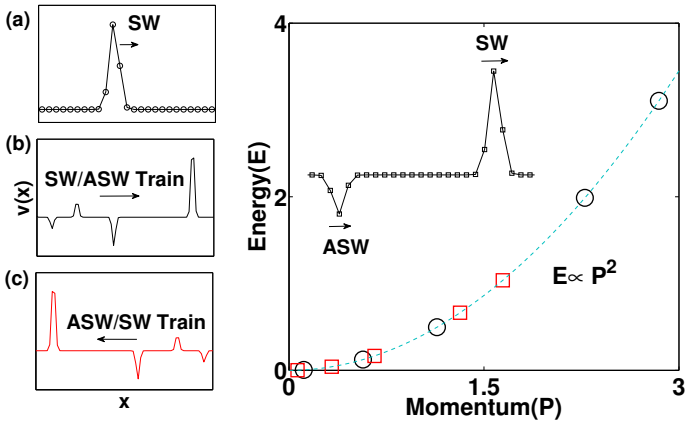

Figure 5.1: *left:*(a) Velocity profile of the compressive solitary wave (SW) generated in an athermal chain of beads with one sided interaction. (b-c) Velocity profiles showing the formation of a train of SW-ASW pair for two-sided non-linear springs. A single particle is initially given an impulse to the right, generating a train led by a SW moving in the direction of the impulse (b), while simulatenously generating a symmetric train led by an ASW moving in the opposite direction. *right:* The energy momentum relation for the leading SW/ASW in the three cases shown in the left panel following the energy (E) momentum (P) relation $E = \frac{P^2}{2m_{eff}}$. *inset*: Zoom in of the leading SW-ASW pair from left panel (b).

5.1 THE ANTI-SOLITON

In Fig. (5.1), we demonstrate that the compressional solitary wave (SW) excitation discovered by Nesterenko in a chain of non-cohesive beads is also seen in a lattice of springs with two sided interactions. However, unlike the case of a one sided potential, each compressive SW generated in response to an impulse is accompanied by a corresponding expansion solitary wave (formed by local stretching of springs) of the same magnitude but moving in the opposite direction. This anti solitary wave (ASW) is not sustained by beads interacting with purely repulsive potentials – the beads would merely loose contact.

The anti-soliton is not sustained by beads interacting with purely repulsive potentials.

In Fig. (5.1) left panel, we show the SW/ASW excitations for (a)beads , (b-c) particles connected by springs. In Fig. (5.1), right panel, we plot the energy-momentum relation for the leading SW/ASW demonstrating that SW excitations in a lattice of repulsive beads have the same effective mass m_{eff} (as defined in Eq. (A.17)) as a SW and ASW in two-sided springs. As shown in Fig. (5.1) left panel (b-c), the leading SW-ASW generated in response to an impulse imparted to one of the particles towards the right (direction of arrow) is followed by a train of alternating SW-ASW's excitations, of progressively smaller magnitudes. The smaller SW/ASW's are generated as the particle initially imparted the impulse, recoils with its left-over energy. This process is repeated several times, leading to the generation of the train of smaller excitations. Since the speed of propagation depends upon the amplitude, the SW and ASW that start propagating together initially (appearing bounded), eventually separate and become clearly distinguishable.

5.2 LANGEVIN EQUATION

The classical energy-momentum relation (see Fig. (5.1) right panel) satisfied by the SW motivates the interpretation of the solitary wave as a quasi-particle [32, 17]. For small perturbations, the SW can still be treated as a quasi-particle provided the effects of the perturbations accrue gradually such that the SW retains its functional form. We now apply this adiabatic approximation to derive an effective Langevin equation for the SW quasi-particle when the lattice of springs is coupled to a

heat bath. Recall first, the Langevin equation for a particle of mass m undergoing Brownian motion in one dimension is

$$\begin{aligned} \frac{dx}{dt} &= v, \\ \frac{dE}{dt} &= -2\frac{\zeta}{m}K + \sqrt{\frac{2\beta^2 K}{dt}}N(0,1). \end{aligned} \tag{5.1}$$

Here, E, K are the total and kinetic energies respectively, ζ, β are the dissipation and diffusion coefficients related via the fluctuation dissipation theorem $\beta^2 = 2\zeta k_B T/m^2$, where k_B is the Boltzmann constant. $N(0,1)$ is a normal random variable with mean 0 and variance 1, and encapsulates the effects of random fluctuations during the time interval $t, t+dt$. For a free particle of unit mass moving with speed v, $E = K = \frac{1}{2}v^2$ and upon substituting in Eq. (5.1), we recover the Langevin's equation conventionally expressed as the rate of change of momentum of the particle [63].

We now derive an equation analogous to Eq. (5.1) for the compressive solitary wave quasi-particle. Identifying the lattice spacing a as a characteristic length scale and $\omega = \sqrt{\frac{k}{m}a^{\alpha-2}}$ as an inverse time scale, the equation of motion for the compressive displacement field $\phi(x,t)$ in dimensionless units reads-

$$\phi_{tt} - \frac{1}{12}\phi_{xxtt} + [(-\phi_x)^{\alpha-1}]_x = 0 \tag{5.2}$$

where subscripts denote partial derivatives with respect to space x and time t. Eq. (5.2) is a simplified form of the Nesterenko equation [32, 49], see Supplementary Information I for details. The first two terms express the rate of change of momentum while the third term represents the force. Although the solitary wave solution to Eq. (5.2) is not exact (lacking compact support), Eq. (5.2) provides a good approximation while being analytically more tractable especially since we are interested in keeping the non-linear exponent α general [49, 26]. Note that the equation for the ASW (stretching) is obtained by modifying the third term $+[(-\phi_x)^{\alpha-1}]_x \to -[(\phi_x)^{\alpha-1}]_x$ in Eq. (5.2). Upon substituting $\delta = -\phi_x$ for the compressive SW or $\delta = \phi_x$ for the expansive ASW, we find the same functional forms for the solitary wave solutions in both cases.

In analogy with the Langevin equation for a particle, we model the coupling to a heat bath as the sum of two contributions-

an external drag and a random fluctuating force, phenomenologically introduced into the equation of motion as :

$$\phi_{tt} - \frac{1}{12}\phi_{xxtt} + [(-\phi_x)^{\alpha-1}]_x = -\gamma\left(\phi_t - \frac{1}{12}\phi_{txx}\right) + \sqrt{\frac{2\gamma}{\alpha\Gamma dt}}\left(\eta(x,t;t+dt) - \frac{1}{\sqrt{12}}\eta_x(x,t;t+dt)\right) \quad (5.3)$$

where $\gamma = \frac{\zeta}{m\omega}$ is the dimensionless drag coefficient that couples to the momentum $\Pi = \left(\phi_t - \frac{1}{12}\phi_{txx}\right)$. It is useful to define a coupling constant $\Gamma = \frac{ka^\alpha}{\alpha k_B T}$ as the ratio of potential to thermal energy in terms of which, the dimensionless diffusion coefficient is $D = \frac{2\gamma}{\alpha\Gamma}$. The last (noise) term on the right of Eq. (5.3) in conjunction with Π, satisfies the fluctuation dissipation theorem [64] (see Supplementary Information 3 for details). Here, $\eta(x,t;t+dt)$ is a Gaussian random noise during the time interval $t, t+dt$ with the moments $\langle\eta(x,t;t+dt)\rangle = 0$ and $\langle\eta(x,t;t+dt)\eta(x',t';t'+dt')\rangle = \delta(x-x')\delta(t-t')$ respectively, where angular brackets denotes ensemble averaging.

To study the propagation of the SW in a background of thermal fluctuations, we now make a working assumption based on the quasi-particle approximation to the SW: whenever the energy of the SW, $E \equiv E_{SW} \gg k_B T$, the SW functional form is unaltered and only its amplitude $A(t)$ becomes time-dependent. The amplitude $A(t)$ is the collective variable for the SW quasiparticle and other properties of the solitary wave, such as its energy and momentum may be determined from it. Note, the width of the SW is independent of its amplitude and therefore we do not consider its time dependence [64].

From Eq. (5.2), the conserved energy is

$$E = \int dx\, \frac{1}{2}\phi_t^2 + \frac{1}{24}\phi_{tx}^2 + \frac{1}{\alpha}(-\phi_x)^\alpha, \quad (5.4)$$

and the energy of the SW may be obtained by integrating Eq. (B.27) over the width of the SW of order W. (This avoids including the energy of small SW that separate from the main wave). Using Eq. (5.2), the rate of change of energy is,

$$\frac{dE}{dt} = \sqrt{\frac{D}{dt}}\int dx\eta(x,t;t+dt)\left(\phi_t + \frac{1}{\sqrt{12}}\phi_{tx}\right) - 2\gamma K \quad (5.5)$$

where, K is the kinetic part of the energy,

$$K = \int dx\, \left(\frac{1}{2}\phi_t^2 + \frac{1}{24}\phi_{tx}^2\right). \quad (5.6)$$

The last term on the right of Eq. (5.5) describes the possible mechanisms of decay of the SW by "friction" from the heat bath (γ). The first term is the fluctuating part of the energy. In the following, we make the assumption (verified numerically) that the coupling to the heat bath is more important and therefore, any drag induced by background phonons is negligible.

Solving for the SW solution from Eq. (5.2), we find $\phi_t = A\psi$, where

$$\psi(x,t) = \operatorname{sech}^{\frac{2}{\alpha-2}}\left(\frac{x - V_s t}{W}\right) \tag{5.7}$$

is the functional form of the SW with amplitude A, speed $V_s = A^{\frac{\alpha-2}{\alpha}}$ and width $W = \frac{1}{\sqrt{3}(\alpha-2)}$ in units of the lattice spacing, see Supplementary Information I for details. The SW energy, kinetic energy, and momentum may now be expressed in terms of the collective variable A:

$$E = A^2 \int dx\, \psi^2(x,t) = A^2 I_E \tag{5.8}$$

and from the the virial theorem,

$$K = \frac{\alpha}{\alpha+2} E = \frac{\alpha}{\alpha+2} I_E A^2 \tag{5.9}$$

Additionally, the solitary wave momentum is

$$P = A \int dx\, \psi(x,t) = A I_P. \tag{5.10}$$

Here,

$$I_E = \int dx\, \operatorname{sech}^{\frac{4}{\alpha-2}}\left(\frac{x}{W}\right) \tag{5.11}$$

$$I_P = \int dx\, \operatorname{sech}^{\frac{2}{\alpha-2}}\left(\frac{x}{W}\right), \tag{5.12}$$

are constants obtained by integrating over all space [49].

Substituting for E and K in terms of A, we cast Eq. (5.5) into the form of an ordinary Langevin equation (with additive noise) for the collective variable $A(t)$,

$$\frac{dA}{dt} = \sqrt{\frac{2\gamma}{\alpha\Gamma I_E^2 A(t)^2 dt}} \int dx\, \eta(x,t;t+dt)\left(\phi_t + \frac{1}{\sqrt{12}}\phi_{tx}\right) - \frac{\alpha\gamma}{\alpha+2}A \tag{5.13}$$

where, $\phi \equiv \phi(x,t)$. Eq. (5.13) is the central result of our work whose analytical predictions we derive and test numerically in

the next sections. The first term can be written as $\frac{1}{\sqrt{dt}}\eta_A(t, t+dt)$, where η_A is a white noise signal; that is, its correlations are given by $\langle \eta_A(t)\eta_A(t')\rangle = \frac{2\gamma}{(\alpha+2)I_E\Gamma}\delta(t-t')$. Using the fact that the correlations of $\eta(x,t)$ are described by delta-functions, the correlations of $\eta_A(t)$ can be related to the kinetic energy Eq. (5.6), which can be replaced by $\frac{\alpha}{\alpha+2}I_E A(t)^2$.

5.3 MEAN AND VARIANCE

Taking the expectation value (ensemble average) of Eq. (5.13), we find

$$\frac{d\langle A\rangle}{dt} = -\frac{\alpha\gamma}{\alpha+2}\langle A\rangle, \tag{5.14}$$

where, owing to the noise term $\eta(x,t;t+dt)$ (which acts between times $t; t+dt$) and $\phi_t(x,t)$ (which is a solution at time t) being statistically independent, the expectation value $\langle \eta(x,t;t+dt)\phi_t(x,t)\rangle = 0$. Consequently, the solitary wave amplitude decays as

$$\langle A\rangle = A_0 e^{-\frac{\alpha\gamma}{\alpha+2}t} \tag{5.15}$$

where, A_0 is the initial solitary wave amplitude. Note, the effective damping rate $\gamma' = -\frac{\alpha\gamma}{\alpha+2}$ is independent of inverse temperature Γ but rescales with the exponent of the non-linear potential α.

Similarly, we solve for the variance of the solitary wave amplitude or equivalently, the variance in the square root of energy. Re-defining, $D = \frac{\gamma}{2\alpha\Gamma I_E^2}$, we solve for the variance in the solitary wave amplitude by first evaluating the differential $d[A^2] = A^2(t+dt) - A^2(t)$, by substituting $A(t+dt) = A(1-\frac{\alpha\gamma}{\alpha+2}dt) + \sqrt{D\,dt}\int dx\ \eta(x,t;t+dt)\left(\psi + \frac{1}{\sqrt{12}}\psi_x\right)$ from Eq. 5.14 and retaining terms to order $0(\sqrt{dt})$[65, 66],

$$\begin{aligned} d[A^2] &= -\frac{2\alpha\gamma}{\alpha+2}A^2 dt + 2A\sqrt{D\,dt}\int dx\eta(x,t;t+dt)\xi(x,t) + \\ &\quad + D\,dt\int\int dx\,dx'\eta(x,t;t+dt)\eta(x',t;t+dt)\xi(x,t)\xi(x',t) \end{aligned} \tag{5.16}$$

where for brevity, we have defined $\xi(x,t) = \left(\psi(x,t) + \frac{1}{\sqrt{12}}\psi_x(x,t)\right)$. Taking the expectation value, the second term on the right van-

ishes (as discussed for the mean) and using the property that the noise term is delta-correlated in space, we obtain

$$\frac{d[\langle A^2\rangle]}{dt} = -\frac{2\alpha\gamma}{\alpha+2}\langle A^2\rangle + D\int dx\ \left(\psi + \frac{1}{\sqrt{12}}\psi_x\right)^2.$$

The last term when expanded gives twice the solitary wave kinetic energy 2K, see Eq. (5.6), plus an integral $\frac{2}{\sqrt{12}}\int dx\psi\psi_x$, that vanishes by symmetry for the SW solution. Moreover, the SW kinetic energy is related to its total energy via the virial relation $K = \frac{\alpha}{\alpha+2}E$. Hence, we obtain the ordinary differential equation correct to order dt -

$$\frac{d\langle A^2\rangle}{dt} = -\frac{2\alpha\gamma}{\alpha+2}\langle A^2\rangle + 2DI_E\frac{\alpha}{\alpha+2}. \tag{5.17}$$

Solving, the differential equation subject to the initial condition $\langle A^2\rangle_{t=0} = A_0^2$ and substituting for D, we obtain,

$$\langle A^2\rangle = A_0^2 e^{-\frac{2\alpha\gamma}{\alpha+2}t} + \frac{1}{2I_E\alpha\Gamma}\left(1 - e^{-\frac{2\alpha\gamma}{\alpha+2}t}\right). \tag{5.18}$$

Using Eq. (5.15), this may be expressed as

$$\mathrm{var}(A) = \langle A^2\rangle - \langle A\rangle^2 = \frac{1}{2I_E\alpha\Gamma}\left(1 - e^{-\frac{2\alpha\gamma}{\alpha+2}t}\right). \tag{5.19}$$

Using the relation in Eq. (5.8), we rewrite the above equation as

$$\mathrm{var}(\sqrt{E}) = \frac{1}{2\alpha\Gamma}\left(1 - e^{-\frac{2\alpha\gamma}{\alpha+2}t}\right). \tag{5.20}$$

The SW quasi-paricle in a background of thermal fluctuations behaves as Brownian particle.

The coefficient $\frac{1}{2\alpha\Gamma}$ reduces to $\frac{k_BT}{2}$ when the energy is not measured in units of $k a^\alpha$, so this expression is analogous to the velocity variance of a Brownian particle. Note, for large α, the SW is effectively one particle wide and thus Eq. (5.20) captures the correct thermal equilibration of the particle energy with the heat bath. However, for the dynamics of the SW, Eq. (5.20) is only useful as long as the SW is identifiable against the background thermal energy, that is $E_{SW} \gg \Gamma^{-1}$.

5.4 SIMULATIONS

We consider a one dimensional chain consisting of $N = 1024$ particles each having a mass m placed regularly on a lattice with spacing a (spring rest length) interacting pair-wise with a

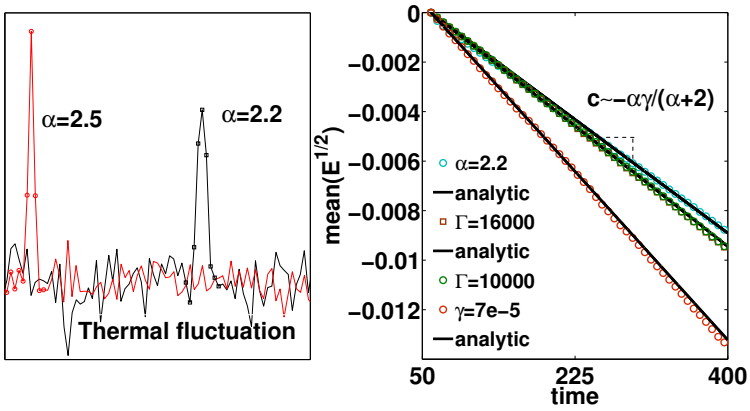

Figure 5.2: *left*: Snapshot of two solitary waves in a background of thermal fluctuations for $\alpha = 2.5$ (red) and $\alpha = 2.2$ (black). *right*: the attenuation of the solitary wave as a function of time for various values of γ,Γ, and α. When not indicated, $\alpha = 2.5, \Gamma = 10^4$ and $\gamma = 5 \times 10^{-}5$. The data for these values is shown with green circles; the other data corresponds to changing one parameter, $\alpha = 2.2$ (black circles), $\Gamma = 1.6\text{x}10^4$, (brown squares) and $\gamma = 7\text{x}10^{-5}$ (red circles) compared with the analytic expression in Eq. (5.15) represented by solid lines. The initial $E_{SW} = 0.5$.

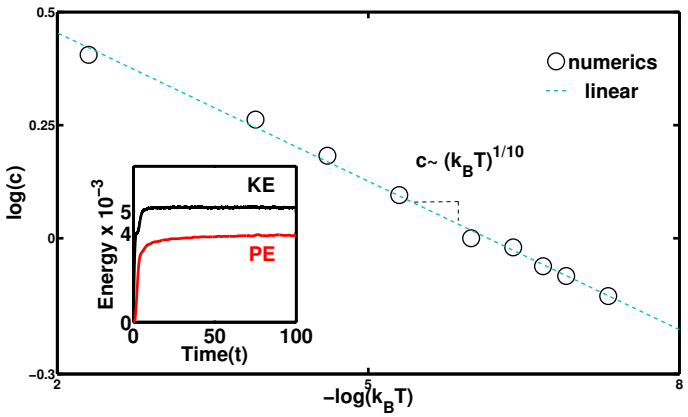

Figure 5.3: The sound speed computed from the dispersion curves for a range of Γ (inverse temperature) for $\alpha = \frac{5}{2}$. The circles are from numerical simulation while the dashed blue line is a linear fit, giving a slope of 0.11 for $\alpha = \frac{5}{2}$, close to the expected value $\frac{\alpha-2}{2\alpha}$. The inset shows the kinetic and potential energy approaching thermal equilibrium, where their ratio satisfies the virial relation KE/PE $= \alpha/2$.

nearest neighbour interaction $V(\delta) = \frac{K}{\alpha}(\delta)^{\alpha}$, where δ is the compression/stretching induced during the dynamics. We model the coupling to the heat bath by numerically integrating Eq. (5.1) for each particle using the predictor-corrector algorithm [71]. In thermal equilibrium the mean kinetic energy is KE$\sim \frac{k_B T}{2}$ and potential energy is PE$\sim \frac{k_B T}{\alpha}$, where their ratio satisfies the virial relation, see Fig. (5.3), inset for $\alpha = 5/2$. In the following, all numerical data is presented in dimensionless units, ensemble averaged over 1000 samples.

5.4.1 *Fluctuation induced rigidity*

To extract the equilibrium properties in the thermalized state, we define the longitudinal current density of particles as $j(x,t) = \frac{1}{\sqrt{N}}\sum_{i=1}^{N} v_i(t)\delta(x - x_i(t))$, and its Fourier transform $j(k,t) = \frac{1}{\sqrt{N}}\sum_{i=1}^{N} v_i(t)e^{ikx}$, where k is the longitudinal collective mode along the x-direction. Thus, the corresponding longitudinal current density auto-correlation functions is $C(k,t) = \langle j^*(k,0)j(k,t)\rangle$, where the angular brackets denote ensemble averaging over the initial time. The longitudinal power spectral density is then obtained as the Fourier transform of the respective current density auto-correlation functions as, $P(k,\omega) = \int_{-\infty}^{\infty} dt\ e^{i\omega t}C(k,t)$. The Fourier transforms defined above are evaluated using fast Fourier transform from simulation data. The sound speeds in Fig. (5.3) correspond to the linear part of the dispersion curves, obtained by projecting the power spectral densities on the frequency (ω)- wavenumber (k) plane. See Supplementary Information C for details.

By coupling a lattice of non-linear springs to a thermal bath, we see the emergence of entropic elasticity.

In Fig. (5.3), we plot the sound speed from the slope of the dispersion curves for $\alpha = 5/2$ for a range of Γ. At thermal equilibrium, the mean kinetic energy and hence the temperature T satisfy the virial relation $T \sim \delta_T^{\alpha}$, where δ_T is the average displacement of the particles induced by thermal fluctuations. Defining the sound speed c as the second derivative of the induced potential energy leads to the relation, $c^2 \sim T^{\frac{\alpha-2}{\alpha}}$ [38]. For $\alpha = \frac{5}{2}$, we find $c \sim \Gamma^{\frac{-1}{10}} \sim (k_B T)^{\frac{1}{10}}$, closely matching the linear fit in Fig. 5.3. Thus, coupling the lattice of non-linear springs that is initially in its state of sonic vacuum (implying the absence of linear sound) to a heat bath, leads to hydrodynamical sound modes with a linear sound speed that scales with the temperature of the heat bath [38]. Note, setting $\alpha = 2$ (harmonic springs) yields a sound speed that is independent

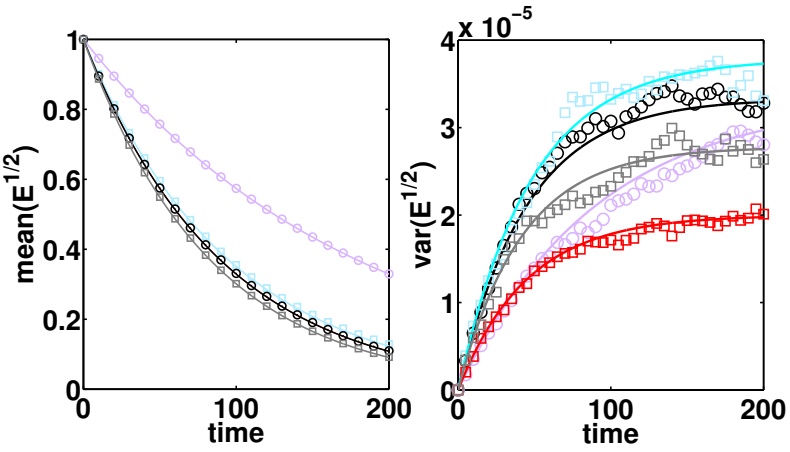

Figure 5.4: *left*: the numerically obtained mean solitary wave energy for $\alpha = 2.5, \gamma = 0.01$ (purple circles), $\alpha = 2.2, \gamma = 0.02$ (blue squares), $\alpha = 2.5, \gamma = 0.02$ (black circles), $\alpha = 3.0, \gamma = 0.02$ (gray squares) decaying exponentially compared against the analytical expression (solid curves). The mean decay rate is independent of the temperature Γ^{-1}. *right*: the numerically obtained varaince of the solitary wave energy for $\alpha = 2.2, \gamma = 0.02, \Gamma = 6000$ (blue squares), $\alpha = 2.5, \gamma = 0.02, \Gamma = 6000$ (black circles), $\alpha = 3.0, \gamma = 0.02, \Gamma = 6000$ (grey squares), $\alpha = 2.5, \gamma = 0.01, \Gamma = 6000$ (purple circles) and $\alpha = 2.5, \gamma = 0.02, \Gamma = 10000$ (red squares) compared against the analytical expression Eq. (5.20) (solid curves).

of temperature while the limit $\alpha \to \infty$ yields $c \sim (k_B T)^{\frac{1}{2}}$, a result in agreement with the entropic elasticity for hard sphere colloidal crystals [52].

5.4.2 *Comparison with analytics*

Once the lattice reaches thermal equilibrium, we excite a solitary wave (SW) by imparting one of the particles an initial energy of order $E_{SW} = 0.5$ in dimensionless units. In Fig. (5.2) left panel, we show a snapshot of two SWs at the same time, propagating in a background of thermal fluctuations for $\alpha = 2.5$ (red) and $\alpha = 2.2$ (black). We see that the SW with lower α is wider and moves faster for the given amplitude, in qualitative agreement with the analytic widths $W \sim \frac{1}{\sqrt{3}(\alpha-2)}$ and speeds $V_s \sim A^{\frac{\alpha-2}{\alpha}}$.

In Fig. (5.4) left panel, we plot the numerical data (symbols) for the attenuation of the SW amplitude as a function of time for various values of γ and α and we find a very good match to the analytic expression in Eq. (5.15) (solid curves). For the range of Γ explored, we find the damping rate is independent of temperature (Γ) but depends on the environmental drag γ and α.

In Fig. (5.4) right panel, we show the increase in the variance of SW amplitude (or the square root of its energy) as a function of time for multiple values of α , γ and Γ obtained numerically (symbols) and compare them with the complete analytical solution Eq.(5.20) finding good agreement. Notice, the final value of the variance correctly approaches the thermal energy, as expected for a Brownian particle. However, since the solitary wave is a dynamical object that decays under the influence of the external drag, once the solitary wave energy becomes comparable to the background thermal energy, it is no longer meaningful to consider it as a Brownian particle.

SHEAR FRONTS IN RANDOM SPRING NETWORKS.

We now shift our attention to another model of fragile matter: a two dimensional disordered network of harmonic springs. At a critical value of its mean connectivity, such a network becomes fragile: it undergoes a rigidity transition signalled by a vanishing shear modulus and transverse sound speed. We then investigate analytically and numerically the linear and non-linear visco-elastic response of these networks by probing the dynamics that result from shearing one edge of the sample at a uniform rate. Similar to our previous studies, we will find that close to the rigidity transition, the regime of linear response becomes vanishingly small and the tiniest shear strains generates non-linear shear shock waves. Moreover, we find that the response of the networks at early times is reminiscent of the emergent fluid like state we saw in Chapter 4. In this case, the emergent viscosity directly manifests in the super-diffusively growing widths of the nonlinear shock front*.

* The research ideas presented in this chapter evolved out of interesting discussions with V. Vitelli and S. Ulrich and are part of Reference [9]. Thanks to S. Ulrich for the simulations and accompanying figures.